

# APPLICATION OF SEVERAL CONTROL TECHNIQUES FOR THE IONOSPHERIC OBSERVATION NANOSATELLITE FORMATION

Bo J. Naasz\*, Christopher D. Karlgaard<sup>†</sup> and Christopher D. Hall <sup>‡</sup>

This paper presents the results of applying several generic control strategies to the problem of maintaining and maneuvering a formation of Earth observing satellites. These standard techniques include both linear and nonlinear control methodologies. The effects of several constraints are considered, including fixed thrust magnitude and non-radial thrusting. In-plane and in-track formation types are discussed in both cooperative and master-slave command and control architectures. Results are compared for a simple anomaly-shift maneuver, and a time-optimal continuous thrust maneuver is used as a baseline for the comparisons.

## INTRODUCTION

In the past ten years, spacecraft formation flight has been the topic of a great deal of research. The motivation for formation flying spacecraft is simply stated: just as geese and military aircraft fly in formation to increase the overall efficiency of the group, so too can spacecraft fly in close formation to increase the overall efficiency, performance, and survivability of a mission.

The Ionospheric Observation Nanosatellite Formation (ION-F) consists of three spacecraft, one each designed and built by students at Virginia Tech, Utah State, and the University of Washington. The mission has three primary objectives: to conduct a multi-point study on properties of the ionosphere;<sup>1</sup> to test and demonstrate the concept of formation flying for use in space missions;<sup>2</sup> and to provide students with the valuable opportunity to design, build, and operate a real spacecraft. ION-F is sponsored by the Air Force and NASA and will launch on the Space Shuttle in 2003.

We begin by describing the spacecraft and its capabilities, and then discuss the modelling choices associated with formation flying simulations. We develop linear and nonlinear control laws and apply them to a control problem of interest for the ION-F mission.

## CONTROL HARDWARE

HokieSat, the Virginia Tech nanosatellite, presents an interesting control problem. A pulsed plasma thruster (PPT) system has been developed specifically for the ION-F mission by the University of Washington and Primex Aerospace Corporation.<sup>3,4</sup> Figure 1 shows the layout of these thrusters in the HokieSat spacecraft. Thrusters  $T_2$  and  $T_3$  in the figure are the primary source of translation control, whereas thrusters  $T_1$  and  $T_4$  provide yaw steering to augment the magnetic torque coil system. The thrusters produce an impulse-bit of 56  $\mu\text{N}\cdot\text{s}$  and fire at a rate of 1 Hz, giving

---

\*Graduate Assistant, Department of Aerospace and Ocean Engineering, Virginia Polytechnic Institute and State University, Blacksburg, Virginia. bo@vt.edu. Student Member AIAA.

<sup>†</sup>Graduate Assistant, Department of Aerospace and Ocean Engineering, Virginia Polytechnic Institute and State University, Blacksburg, Virginia. Currently, Project Engineer, Analytical Mechanics Associates, Inc., Hampton, Virginia. karlgaard@ama-inc.com. Member AIAA, Member AAS.

<sup>‡</sup>Associate Professor, Department of Aerospace and Ocean Engineering, Virginia Polytechnic Institute and State University, Blacksburg, Virginia. cdhall@vt.edu. Associate Fellow AIAA, Member AAS.

a total translational impulse-bit of  $112 \mu\text{N}\cdot\text{s}$ . As there are no thrusters pointed in the zenith-nadir direction, and the spacecraft must remain nadir-pointing for inter-satellite communications, radial thrusting is prohibited.

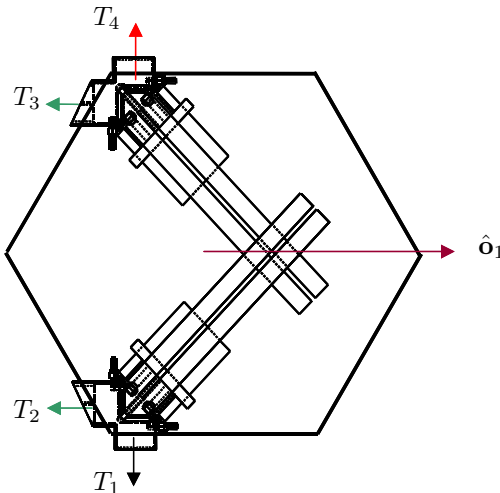


Figure 1: HokieSat pulsed plasma thruster (PPT) layout viewed from zenith direction

The attitude determination and control system of HokieSat is described in Ref. 5. The attitude is primarily controlled by a system of magnetic torque coils, with thrusters  $T_1$  and  $T_4$  providing a level of redundancy for yaw steering. For the preliminary formation control laws described in this paper we assume that the spacecraft can be slewed in order to provide thrust in any allowable direction. Specifically, we do not allow thrust in the radial direction, since the spacecraft does not have thrusters mounted on the nadir or zenith faces and must remain nadir-pointing.

All of the ION-F spacecraft use a combined GPS-based navigation and crosslink communications system designed and manufactured by the Applied Physics Laboratory.<sup>6</sup> This system allows each spacecraft to determine its orbit and communicate this and other information to the other spacecraft allowing for autonomous operations.

Additional information about the HokieSat spacecraft may be found in Ref. 7.

## MODELLING OF FORMATION FLIGHT

The ION-F formation flying mission includes two simple formation types: the anomaly shift formation, and the same ground track formation, both illustrated in Fig. 2. The anomaly shift formation consists of two or more spacecraft in identical orbits separated by some change in true anomaly,  $\delta\nu$ .

The same ground track formation consists of two or more spacecraft orbits separated by shifts in true anomaly,  $\delta\nu$ , and right ascension,  $\delta\Omega$ . The value of  $\delta\Omega$  orients the orbits so that all of the spacecraft in the formation share the same ground track:

$$\delta\Omega = \omega_e \delta t \tag{1}$$

where  $\omega_e$  and  $\delta t$  are the angular velocity of the Earth and the time between satellite ground passes, respectively.

Figure 3 shows three models for controlling and simulating formation dynamics. The three models increase in complexity from a simple rendezvous problem to a cooperative, multi-craft maneuvering problem. The rendezvous problem is the problem of maneuvering the active spacecraft to rendezvous with a point relative to the passive spacecraft.

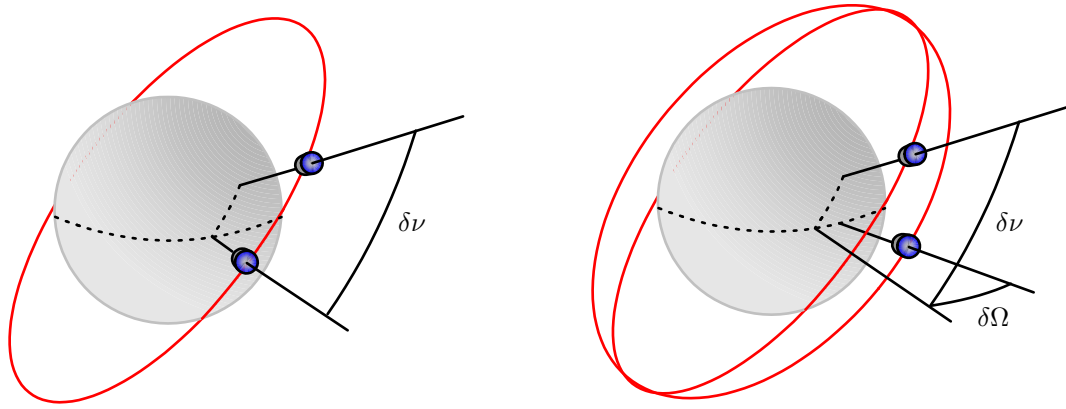


Figure 2: Anomaly shift and same ground track formations

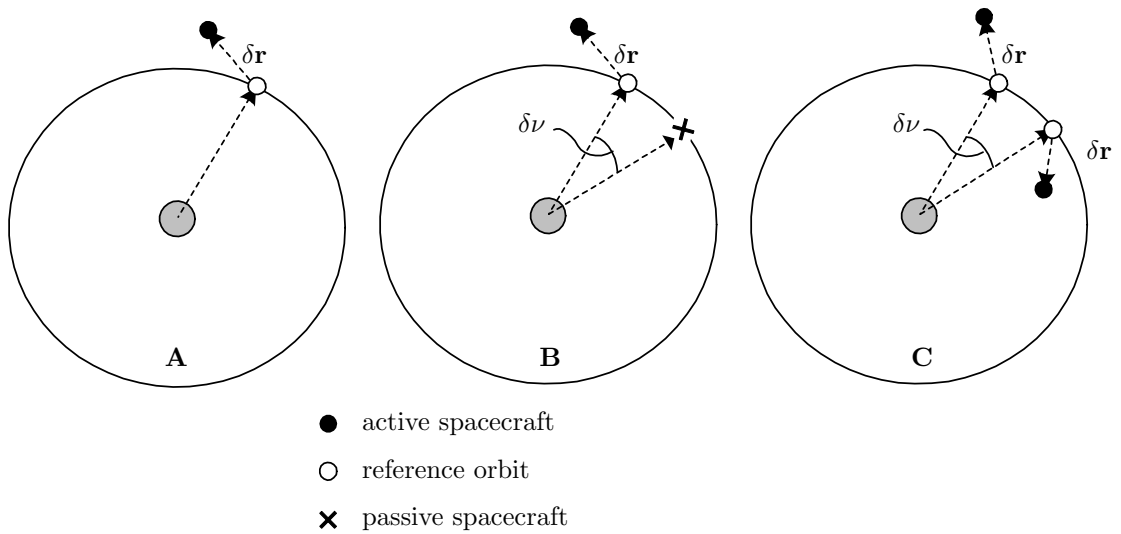


Figure 3: Formation simulation models: **A)** rendezvous model; **B)** leader-follower model; **C)** cooperative model

The intermediate model is a leader-follower (or master-slave) type formation where the reference orbit of the active spacecraft (the follower) is determined by a formation planner from the leader's orbit. In the case of an anomaly shift formation, the active spacecraft targets a reference orbit defined by a  $\delta\nu$  shift of the leader's orbit. This model is only required if differential perturbations, such as Earth oblateness or orbit control at the leader spacecraft, are applied, causing the reference orbit to drift with respect to the leader's. If no perturbations are applied in orbit propagation, this model is identical to the target-interceptor problem, as the reference orbit follows a path identical to the leader's.

The cooperative, multi-craft maneuvering problem involves the complicated task of determining reference orbits for two active spacecraft from the inertial orbits of the two spacecraft, and a predetermined relative formation type. In Ref. 8, the authors show that the use of two actively controlled spacecraft as opposed to a leader-follower type formation improves the efficiency of formation control by minimizing both the time and the number of thrust impulses required to establish the desired formation.

The desired relative orbit can be chosen in many ways, possibly to optimize the mission per-

formance in some sense,<sup>9</sup> or to minimize the effect of gravitational perturbations on the formation geometry<sup>10</sup> in an effort to minimize formation-keeping propellant consumption. In the study presented here, only the anomaly shift and same ground track formations are considered.

The standard Earth-centered inertial frame is designated as  $\mathcal{F}_i$  and has unit vectors  $\hat{\mathbf{i}}_1$ ,  $\hat{\mathbf{i}}_2$  and  $\hat{\mathbf{i}}_3$  in the inertial  $x$ ,  $y$  and  $z$  directions, respectively. The perifocal frame,  $\mathcal{F}_p$  has unit vectors  $\hat{\mathbf{p}}_1$ ,  $\hat{\mathbf{p}}_2$  and  $\hat{\mathbf{p}}_3$  with  $\hat{\mathbf{p}}_1$  in the periapsis direction,  $\hat{\mathbf{p}}_3$  in the orbit normal direction, and  $\hat{\mathbf{p}}_2 = \hat{\mathbf{p}}_3 \times \hat{\mathbf{p}}_1$ . The orbit frame,  $\mathcal{F}_o$ , has unit vectors  $\hat{\mathbf{o}}_1$ ,  $\hat{\mathbf{o}}_2$  and  $\hat{\mathbf{o}}_3$  with  $\hat{\mathbf{o}}_3$  in the nadir direction,  $\hat{\mathbf{o}}_2$  in the direction of the negative orbit normal, and  $\hat{\mathbf{o}}_1 = \hat{\mathbf{o}}_2 \times \hat{\mathbf{o}}_3$ , which is the velocity direction for a circular orbit. The spherical frame,  $\mathcal{F}_s$ , is a permutation of the orbital frame, and has unit vectors  $\hat{\mathbf{s}}_1$  in the radial direction,  $\hat{\mathbf{s}}_2$  in the velocity direction and  $\hat{\mathbf{s}}_3$  in the orbit normal direction.

The equations of motion for a point-mass satellite take the form

$$\ddot{\mathbf{r}} = -\frac{\mu}{\|\mathbf{r}\|^3}\mathbf{r} + \vec{\mathbf{a}}_p \quad (2)$$

where  $\mathbf{r}$  is the position vector of the satellite measured from the center of mass of the primary body,  $\mu$  is the gravitational parameter of that body, and  $\vec{\mathbf{a}}_p$  includes perturbation accelerations caused by oblateness effects of the body, atmospheric drag, third body effects and so on. If  $\vec{\mathbf{a}}_p = \mathbf{0}$  then the equations of motion reduce to the ideal Keplerian situation where the body is a perfect sphere and all other disturbances are zero.

## LINEAR CONTROL

Among the more recent developments of linear optimal control are the  $H_2$  and  $H_\infty$  control synthesis techniques.  $H_2$  control is a generalization of the linear quadratic regulator (LQR) method, and  $H_\infty$  methods are based on robustness ideas, but can also be formulated in a linear-quadratic framework through the application of game theory. A brief summary of these methods is given below, but more details may be found in Ref. 11.

$H_2$  control is based on the linear quadratic regulator (LQR) concept, where the control of a linear system is found by seeking the minimum of a real scalar quadratic cost function. The  $H_2$ -optimal control results from including random disturbance inputs modelled as white noise in the LQR problem. This control is also often called the stochastic regulator or the linear quadratic Gaussian (LQG) control. For full-information state-feedback problems, the  $H_2$  control design reduces to an equivalent state-feedback LQR solution.<sup>11</sup>

$H_\infty$  control results from considering the same type of problems as encountered in the  $H_2$  control problem, but now seeks to minimize the  $\infty$ -norm of the system response. The small gain theorem states that the stability margins of a system are inversely proportional to the maximum singular value, or the  $\infty$ -norm, of the closed loop transfer function from the disturbance input to output. Therefore, stability margins of the closed loop system may be maximized by minimizing the  $\infty$ -norm of that system. In other words,  $H_\infty$  techniques seek to minimize the effect of modelling error on the system stability.

For the case of the control of satellite formations, these techniques use a linearized form of Eq. (2), which, for large deviations from the reference conditions, constitute a poor approximation of the dynamics of satellite motion. In an extremely crude sense, the true dynamics of the system can be thought of as random from the viewpoint of the control system, lending itself well to an  $H_2$  design approach. However, it is better to think of the actual dynamics as truncation error made during the linearization process, leading to the view that  $H_\infty$  is the best approach for this problem since it will minimize the effect of this error.

Linear-quadratic techniques have been applied to the orbital maneuvering and formation control problem by several authors.<sup>12-20</sup> In all of these cases, LQ techniques have proven to be an adequate approach to both formation keeping as well formation maneuvering. Significant gains in performance and robustness, however, may be found by considering an  $H_\infty$  approach.

For this problem, the governing linear equations of motion are the well known Clohessy-Wiltshire equations.<sup>21</sup> The non-dimensional equations of motion expressed in a spherical coordinate system (using the same notation as Ref. 22), subjected to an impulse at non-dimensional time  $\tau_0$  are:

$$\Delta \hat{r}' = \Delta \hat{v}_r \quad (3)$$

$$\Delta \hat{\theta}' = \Delta \hat{\omega}_\theta \quad (4)$$

$$\Delta \hat{\phi}' = \Delta \hat{\omega}_\phi \quad (5)$$

$$\Delta \hat{v}_r' = 3\Delta \hat{r} + 2\Delta \hat{\omega}_\theta \quad (6)$$

$$\Delta \hat{\omega}_\theta' = -2\Delta \hat{v}_r + f_\theta \delta(\tau - \tau_0) \quad (7)$$

$$\Delta \hat{\omega}_\phi' = -\Delta \hat{\phi} + f_\phi \delta(\tau - \tau_0) \quad (8)$$

where  $f_\theta$  and  $f_\phi$  are the components of the impulse and  $\delta$  is the unit impulse function. Note that a radial component of the impulse does not appear, since thrusting is not allowed in that direction. It is easy to verify that this system is controllable in the sense described in Ref. 23 without radial thrust inputs. The equations of motion may be re-dimensionalized by using length units equal to  $r_0$ , the radius of the reference orbit, and time units equal to  $1/\omega_0$ , where  $\omega_0$  is the mean motion of the reference orbit. The solution of this system with the initial conditions  $\Delta \hat{r}(\tau_0)$ ,  $\Delta \hat{\theta}(\tau_0)$ ,  $\Delta \hat{\phi}(\tau_0)$ ,  $\Delta \hat{v}_r(\tau_0)$ ,  $\Delta \hat{\omega}_\theta(\tau_0)$  and  $\Delta \hat{\omega}_\phi(\tau_0)$  is

$$\begin{aligned} \Delta \hat{r}(\tau) = & [4 - 3 \cos(\tau - \tau_0)] \Delta \hat{r}(\tau_0) + \sin(\tau - \tau_0) \Delta \hat{v}_r(\tau_0) \\ & + 2[1 - \cos(\tau - \tau_0)] [\Delta \hat{\omega}_\theta(\tau_0) + f_\theta] \end{aligned} \quad (9)$$

$$\begin{aligned} \Delta \hat{\theta}(\tau) = & 6[\sin(\tau - \tau_0) - (\tau - \tau_0)] \Delta \hat{r}(\tau_0) + \Delta \hat{\theta}(\tau_0) + 2[\cos(\tau - \tau_0) - 1] \Delta \hat{v}_r(\tau_0) + \\ & + [4 \sin(\tau - \tau_0) - 3(\tau - \tau_0)] [\Delta \hat{\omega}_\theta(\tau_0) + f_\theta] \end{aligned} \quad (10)$$

$$\Delta \hat{\phi}(\tau) = \cos(\tau - \tau_0) \Delta \hat{\phi}(\tau_0) + \sin(\tau - \tau_0) [\Delta \hat{\omega}_\phi(\tau_0) + f_\phi] \quad (11)$$

$$\Delta \hat{v}_r(\tau) = 3 \sin(\tau - \tau_0) \Delta \hat{v}_r(\tau_0) + \cos(\tau - \tau_0) \Delta \hat{v}_r(\tau_0) + 2 \sin(\tau - \tau_0) [\Delta \hat{\omega}_\theta(\tau_0) + f_\theta] \quad (12)$$

$$\begin{aligned} \Delta \hat{\omega}_\theta(\tau) = & 6[\cos(\tau - \tau_0) - 1] \Delta \hat{r}(\tau_0) - 2 \sin(\tau - \tau_0) \Delta \hat{v}_r(\tau_0) \\ & + [4 \cos(\tau - \tau_0) - 3] [\Delta \hat{\omega}_\theta(\tau_0) + f_\theta] \end{aligned} \quad (13)$$

$$\Delta \hat{\omega}_\phi(\tau) = -\sin(\tau - \tau_0) \Delta \hat{\phi}(\tau_0) + \cos(\tau - \tau_0) [\Delta \hat{\omega}_\phi(\tau_0) + f_\phi] \quad (14)$$

A discrete representation of the dynamics is better suited for use within a control law development for this problem as it captures the pulsed nature of the thrusters. Such a representation may be found by modelling the dynamics with difference equations rather than differential equations. This transformation can be accomplished by letting  $\tau_0 = k\bar{\tau}$  and  $\tau = (k+1)\bar{\tau}$ , where  $k$  is an integer and  $\bar{\tau}$  is the non-dimensional sampling period between thruster pulses. The equations of motion may be written as

$$\mathbf{x}_{k+1} = A\mathbf{x}_k + B\mathbf{u}_k + \frac{1}{\gamma}\mathbf{w}_k \quad (15)$$

where  $\mathbf{x}_k^T = \{\Delta \hat{r}(k\bar{\tau}), \Delta \hat{\theta}(k\bar{\tau}), \Delta \hat{\phi}(k\bar{\tau}), \Delta \hat{v}_r(k\bar{\tau}), \Delta \hat{\omega}_\theta(k\bar{\tau}), \Delta \hat{\omega}_\phi(k\bar{\tau})\}$ ,  $\mathbf{u}_k^T = \{f_\theta, f_\phi\}$ ,  $\mathbf{w}_k$  is a disturbance input used to model process noise,  $\gamma$  is a scaling parameter which is discussed below, and

$$A = \begin{bmatrix} 4 - 3 \cos \bar{\tau} & 0 & 0 & \sin \bar{\tau} & 2(1 - \cos \bar{\tau}) & 0 \\ -6(\bar{\tau} - \sin \bar{\tau}) & 1 & 0 & 2(1 - \cos \bar{\tau}) & 4 \sin \bar{\tau} - 3\bar{\tau} & 0 \\ 0 & 0 & \cos \bar{\tau} & 0 & 0 & \sin \bar{\tau} \\ 3 \sin \bar{\tau} & 0 & 0 & \cos \bar{\tau} & 2 \sin \bar{\tau} & 0 \\ -6(1 - \cos \bar{\tau}) & 0 & 0 & -2 \sin \bar{\tau} & 4 \cos \bar{\tau} - 3 & 0 \\ 0 & 0 & -\sin \bar{\tau} & 0 & 0 & \cos \bar{\tau} \end{bmatrix} \quad (16)$$

$$B = \begin{bmatrix} 2(1 - \cos \bar{\tau}) & 0 \\ 4 \sin \bar{\tau} - 3\bar{\tau} & 0 \\ 0 & \sin \bar{\tau} \\ 2 \sin \bar{\tau} & 0 \\ 4 \cos \bar{\tau} - 3 & 0 \\ 0 & \cos \bar{\tau} \end{bmatrix} \quad (17)$$

The  $H_2$  and  $H_\infty$  controls developed in this section seek to minimize a cost function in order to regulate the variable  $\mathbf{z}_k = \{Q\mathbf{x}_k, \mathbf{u}_k\}^T$ , where  $Q$  is a weighting matrix that can be scaled in order to shift the emphasis between the state and the control. The infinite-horizon LQR or state-feedback  $H_2$  control seeks to minimize the cost function

$$J_{H_2} = \sum_{k=0}^{\infty} [\mathbf{x}_k^T Q^T Q \mathbf{x}_k + \mathbf{u}_k^T \mathbf{u}_k] \quad (18)$$

which leads to the optimal feedback control<sup>23</sup>

$$\mathbf{u}_k = -(I + B^T P B)^{-1} B^T P A \mathbf{x}_k \quad (19)$$

where matrix  $P$  is determined by solving the discrete algebraic Riccati equation:

$$P = Q^T Q + A^T P A - A^T P B (I + B^T P B)^{-1} B^T P A \quad (20)$$

The  $H_\infty$  optimization problem seeks to achieve a bound on the norm  $\frac{1}{\gamma} \|T(s)\|_\infty < 1$  where  $T(s)$  is the closed loop transfer function matrix from the noise input to output and  $\gamma > 0$  is a bound on the norm which should be made as small as possible. This optimization problem may be restated as a linear-quadratic discrete game by the cost function

$$J_{H_\infty} = \sum_{k=0}^{\infty} \left[ \mathbf{x}_k^T Q^T Q \mathbf{x}_k + \mathbf{u}_k^T \mathbf{u}_k - \frac{1}{\gamma^2} \mathbf{w}_k^T \mathbf{w}_k \right] \quad (21)$$

where the  $H_\infty$ -optimal control is found by minimizing  $J_{H_\infty}$  with respect to  $\mathbf{u}_k$  and maximizing  $J_{H_\infty}$  with respect to  $\mathbf{w}_k$ . This condition means that the optimal control is found in such a way that the plant is stabilized even for the worst possible disturbance or modelling error. The infinite-horizon, state-feedback control for this problem is given in Ref. 24 and is identical in form to Eq. (19), with a modified Riccati equation for matrix  $P$ :

$$P = Q^T Q + A^T P A - A^T P B (I + B^T P B)^{-1} B^T P A + \frac{1}{\gamma^2} P \left( I + \frac{1}{\gamma^2} P \right)^{-1} P \quad (22)$$

Note that as  $\gamma \rightarrow \infty$ , the  $H_\infty$  solution approaches the  $H_2$  solution, meaning that once the scheme for computing the  $H_\infty$  solution has been implemented, it is simple to develop an  $H_2$  solution in tandem once the weighting matrices have been chosen.

## NONLINEAR CONTROL

Whereas linear control techniques can be highly effective in the control of nonlinear systems, nonlinear control strategies can be beneficial in a variety of ways. For example, nonlinear controllers may: a) increase the region of state space in which we can effectively control the system, b) improve control robustness to parametric uncertainty, c) obtain truer optimality results, d) enable control of systems which are not linearly controllable, and e) allow us to preserve and exploit physical insight.

### Lyapunov Control

The direct method, or second method, of Lyapunov is a valuable tool in the analysis of both linear and non-linear systems. The stability of the system

$$\dot{\mathbf{z}} = \mathbf{f}(\mathbf{z}) \quad (23)$$

where

$$\mathbf{z} = \mathbf{x} - \mathbf{x}^* \quad (24)$$

is analyzed using Lyapunov's stability approach by constructing an energy-like scalar Lyapunov function of the state,  $V(\mathbf{z})$ . For such a system, the equilibrium point,  $\mathbf{x}^*$ , is globally asymptotically stable if there is a  $V(\mathbf{z})$ , continuous in the 1<sup>st</sup> derivative, that satisfies the following conditions:<sup>25-27</sup>

$$\begin{aligned} V(\mathbf{0}) &= 0 \\ V(\mathbf{z}) &> 0 \quad \forall \mathbf{z} \neq \mathbf{0} \\ \dot{V}(\mathbf{z}) &< 0 \quad \forall \mathbf{z} \neq \mathbf{0} \\ \lim_{\|\mathbf{z}\| \rightarrow \infty} V &= \infty \end{aligned} \quad (25)$$

While there is no foolproof method for generating Lyapunov functions, quadratic and logarithmic forms are often effective starting points for a trial-and-error approach.

*Cartesian Lyapunov Control.* To implement a cartesian Lyapunov control, we choose a quadratic Lyapunov function,  $V(\mathbf{x})$ , that satisfies the Lyapunov criteria for guaranteed asymptotic stability, where  $\mathbf{x}$  is the inertial, cartesian, state-error vector.

Taking the time derivative of  $V$ , and writing  $\dot{\mathbf{x}}$  as a vector function,  $\mathbf{f}$ , of  $\mathbf{x}$ , and the control,  $\mathbf{u}$ , we get

$$\dot{V} = \frac{\partial V}{\partial \mathbf{x}} \dot{\mathbf{x}} = \frac{\partial V}{\partial \mathbf{x}} \mathbf{f}(\mathbf{x}, \mathbf{u}) \quad (26)$$

To drive the position and velocity error of a formation flying satellite to zero, we define the state vector  $\mathbf{x}$  as

$$\mathbf{x} = \begin{bmatrix} \delta \mathbf{r} \\ \delta \mathbf{v} \end{bmatrix} \quad (27)$$

where  $\delta(\cdot)$  describes the relative value of parameters of the controlled satellite with respect to the reference, or target satellite (in this case, the relative position and velocity):

$$\delta(\cdot) = (\cdot)_{\text{controlled}} - (\cdot)_{\text{reference}} \quad (28)$$

Note here that the *reference* refers to the desired state of the controlled spacecraft, which is calculated from the state of the uncontrolled spacecraft.

We choose a positive definite Lyapunov function,  $V$ , as shown in Eq. (29), so that  $\dot{V}$  can only be negative for decreasing state vector magnitudes:

$$V(\delta \mathbf{r}, \delta \mathbf{v}) = \frac{1}{2} k_1 \delta \mathbf{r}^T \delta \mathbf{r} + \frac{1}{2} k_2 \delta \mathbf{v}^T \delta \mathbf{v} \quad (29)$$

The time derivative of this Lyapunov function is

$$\dot{V}(\delta \mathbf{r}, \delta \mathbf{v}) = [k_1 \delta \mathbf{r} + k_2 \delta \mathbf{v}]^T \delta \mathbf{f} \quad (30)$$

We now have an equation for the Lyapunov function in terms of the relative position and velocity, and the vector function  $\delta \mathbf{f}$ :

$$\delta \mathbf{f}(\mathbf{x}, \mathbf{u}) = \begin{bmatrix} \delta \mathbf{f}_r \\ \delta \mathbf{f}_v \end{bmatrix} \quad (31)$$

The time rate of change of the relative position,  $\delta \mathbf{r}$ , is simply the relative velocity:

$$\delta \mathbf{f}_r = \delta \dot{\mathbf{r}} = \delta \mathbf{v} \quad (32)$$

Similarly, the time rate of change of the relative velocity,  $\delta\mathbf{v}$ , is the relative acceleration, plus the control acceleration. The control term shows up only in the  $\delta\mathbf{f}_v$  equation:

$$\delta\mathbf{f}_v = \delta\ddot{\mathbf{r}} + \mathbf{u} = \ddot{\mathbf{r}} - \ddot{\mathbf{r}}_{\text{ref}} + \mathbf{u} = -\mu \left( \frac{\mathbf{r}}{r^3} - \frac{\mathbf{r}_{\text{ref}}}{r_{\text{ref}}^3} \right) + \mathbf{u} \quad (33)$$

Re-writing Eq. (30), we get

$$\dot{V}(\delta\mathbf{r}, \delta\mathbf{v}) = k_1 \delta\mathbf{r}^T \delta\mathbf{v} + k_2 \delta\mathbf{v}^T \delta\mathbf{f}_v \quad (34)$$

To control the system we must choose a control that cancels the position error from Eq. (32), cancels the relative gravitational force from Eq. (33), satisfies Eq. (35), and satisfies the original criteria for guaranteed asymptotic stability given by Eq. (25):

$$\dot{V}(\delta\mathbf{r}, \delta\mathbf{v}) = -k\delta\mathbf{v}^T \delta\mathbf{v} < 0 \quad (35)$$

A cartesian Lyapunov control acceleration that satisfies these requirements is:

$$\mathbf{u}_{\text{cart}} = \mu \left( \frac{\mathbf{r}}{r^3} - \frac{\mathbf{r}_{\text{ref}}}{r_{\text{ref}}^3} \right) - \frac{k_1}{k_2} \delta\mathbf{r} - k_3 \delta\mathbf{v} \quad (36)$$

Notice that substituting the Lyapunov control,  $\mathbf{u}_{\text{cart}}$ , into  $\delta\mathbf{f}_v$  in Eq. (34) gives the negative-definite derivative required in Eq. (35).

The control given in Eq. (36) has three components, easily distinguishable as a nonlinear dynamics component, and proportional and derivative components. The non-linear dynamics component,  $\mathbf{u}_{\text{dyn}}$ , given by

$$\mathbf{u}_{\text{dyn}} = \mu \left( \frac{\mathbf{r}}{r^3} - \frac{\mathbf{r}_{\text{ref}}}{r_{\text{ref}}^3} \right) \quad (37)$$

negates the relative natural dynamics, allowing the remaining components to behave as a simple proportional-derivative (PD) control. Note that in the control definition, only the PD components have associated gains. This property of the control law means that we can only guarantee asymptotic stability with this controller if the entire  $\mathbf{u}_{\text{dyn}}$  component is applied. This fact is critical when we apply this control law in fixed thrust magnitude problems. When scaling the control acceleration given by Eq. (36), we only have the freedom to scale the proportional and derivative components by choosing appropriate gains. For this reason it is convenient to redefine the cartesian Lyapunov control as:

$$\mathbf{u}_{\text{cart}} = \mathbf{u}_{\text{dyn}} + S\hat{\mathbf{u}}_{\text{PD}} = \mu \left( \frac{\mathbf{r}}{r^3} - \frac{\mathbf{r}_{\text{ref}}}{r_{\text{ref}}^3} \right) + S \left( \frac{-k_P \delta\mathbf{r} - k_D \delta\mathbf{v}}{\| -k_P \delta\mathbf{r} - k_D \delta\mathbf{v} \|} \right) \quad (38)$$

where PD gains,  $k_P$  and  $k_D$ , and scaling factor  $S$  are chosen by the control designer. We introduce the scaling factor as a third gain so that the control can be scaled as needed without changing the ratio of the PD gains, or scaling the  $\mathbf{u}_{\text{dyn}}$  component. Figure 4 illustrates one possible scaling method for a sample formation maneuver in which the magnitude of  $\mathbf{u}_{\text{dyn}}$  is less than the available thrust acceleration,  $T/m$ . The dotted circle in the figure represents the available thrust acceleration. Sketch A in the figure shows an improperly scaled control vector,  $\mathbf{u}_{\text{cart}}$ , in which the entire control is scaled. Sketch B shows an appropriately scaled thrust vector in which the scaling factor,  $S$ , is computed using the law of cosines:

$$\left( \frac{T}{m} \right)^2 = S^2 + \mathbf{u}_{\text{cart}}^2 - 2S\mathbf{u}_{\text{cart}} \cos \theta \quad (39)$$

where

$$\theta = \pi - \cos^{-1} \left( \hat{\mathbf{u}}_{\text{dyn}} \cdot \hat{\mathbf{u}}_{\text{PD}} \right) \quad (40)$$

and thus

$$S = \frac{1}{2} \left[ 2u_{\text{cart}} \cos \theta \pm \sqrt{(u_{\text{cart}})^2 - 4 \left( u_{\text{dyn}}^2 - \left( \frac{T}{m} \right)^2 \right)} \right] \quad (41)$$

When applied to formation maneuvers in which  $\mathbf{u}_{\text{dyn}}$  is negligible, the control law given by Eq. (38) behaves identically to a PD control. As the size of formation maneuvers increase, the  $\mathbf{u}_{\text{dyn}}$  component of the control becomes critical to the success of the maneuver. Problems arise in the application of this control when the  $\mathbf{u}_{\text{dyn}}$  component of the requested control becomes larger than the available thruster acceleration. If the thrusters are incapable of negating the differential acceleration because they cannot provide sufficient thrust, or the maneuver is too large, the cartesian Lyapunov control will not successfully complete the maneuver, and another control law must be employed.

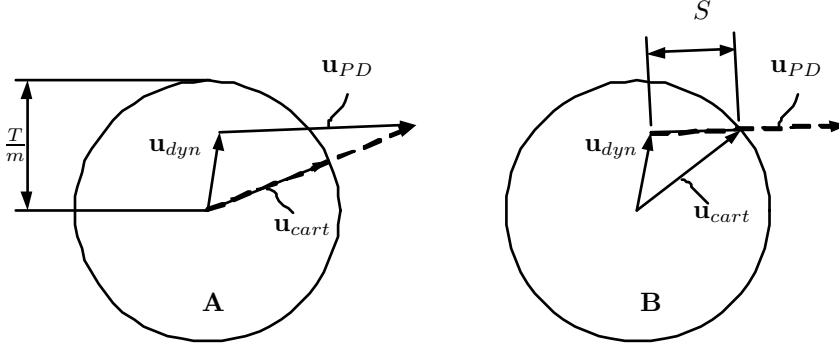


Figure 4: Cartesian Lyapunov control scaling techniques: A) incorrectly scaled control vector; B) properly scaled control vector

*Orbital Element Lyapunov Control.* Schaub and Alfriend<sup>10,28</sup> have shown that Lyapunov control based on orbital element feedback performs well in low-thrust, multi-orbit maneuvers. Unfortunately, the equations of motion required in the development of their Lyapunov control contain singularities for circular, and equatorial orbits. To resolve this issue, we develop a Lyapunov feedback control law using the nonsingular, equinoctial variables.

Ilgen<sup>29</sup> develops Lyapunov optimal feedback control techniques for low thrust orbit transfer between orbits of different semi-major axis, eccentricity, and inclination using both classic, and equinoctial element sets. While the author does not discuss formation-flying control directly, the paper provides an excellent starting point for the development of an equinoctial, Lyapunov-optimal, formation flying feedback control law.

In a straightforward expansion of Ilgen's work, we develop a technique to control the full, six element relative motion of formation flying spacecraft in both classical and equinoctial orbital element forms. For systems of the form

$$\dot{\mathbf{x}} = [\mathbf{g}(\mathbf{x})]\mathbf{u} \quad (42)$$

we can write the derivative as

$$\frac{d}{dt} [V(\mathbf{x} - \mathbf{x}^*)] = \dot{V}(\mathbf{x} - \mathbf{x}^*) = \frac{\partial V}{\partial \mathbf{x}} \dot{\mathbf{x}} = \frac{\partial V}{\partial \mathbf{x}} [\mathbf{g}(\mathbf{x})]\mathbf{u} = V_{\mathbf{x}}[\mathbf{g}(\mathbf{x})]\mathbf{u} \quad (43)$$

Setting the control,  $\mathbf{u}$ , to be

$$\mathbf{u} = -\mathbf{K}[\mathbf{g}(\mathbf{x})]^T V_{\mathbf{x}}^T \quad (44)$$

where  $\mathbf{K}$  is a positive definite gain matrix, the derivative becomes

$$\dot{V}(\mathbf{x}) = -V_{\mathbf{x}}[\mathbf{g}(\mathbf{x})][\mathbf{K}[\mathbf{g}(\mathbf{x})]^T V_{\mathbf{x}}^T] = -\mathbf{K} |[\mathbf{g}(\mathbf{x})]^T V_{\mathbf{x}}^T|^2 \quad (45)$$

This derivative is negative-definite, and therefore, by Lyapunov's second method, the system described in Eq. (42) is globally, asymptotically stable when the control given in Eq. (44) is applied, provided we choose an appropriate positive-definite Lyapunov function.

Gauss's form of Lagrange's Planetary Equations (LPE) takes the form

$$\dot{\mathbf{x}} = \mathbf{f}(\mathbf{x}, \mathbf{u}) = [\mathbf{g}(\mathbf{x})]\mathbf{u} + \mathbf{h}(\mathbf{x}) \quad (46)$$

where  $\mathbf{x}$  is the  $[6 \times 1]$  classical element set,  $[a, e, i, \Omega, \omega, M]$ ,  $\mathbf{u}$  is a  $[3 \times 1]$  control acceleration vector in Hill's frame, and  $\mathbf{f}(\mathbf{x}, \mathbf{u})$  is

$$\mathbf{f}(\mathbf{x}, \mathbf{u}) = \begin{bmatrix} \frac{2a^2 e S \nu}{h} & \frac{2a^2 p}{hr} & 0 \\ \frac{p S \nu}{h} & \frac{(p+r)C\nu+re}{h} & 0 \\ 0 & 0 & \frac{rC(\omega+\nu)}{h} \\ 0 & 0 & \frac{rS(\omega+\nu)}{h} \\ -\frac{pC\nu}{he} & \frac{(p+r)S\nu}{he} & -\frac{hSi}{rS(\omega+\nu)Ci} \\ \frac{b(pC\nu-2re)}{ahe} & -\frac{b(p+r)S\nu}{ahe} & 0 \end{bmatrix} \begin{bmatrix} u_r \\ u_\theta \\ u_h \end{bmatrix} + \begin{bmatrix} 0 \\ 0 \\ 0 \\ 0 \\ 0 \\ n \end{bmatrix} \quad (47)$$

where the sine and cosine functions are abbreviated as  $s(\cdot)$  and  $c(\cdot)$ .

We can modify these equations of motion to match the form of Eq. (42) by replacing the mean anomaly,  $M$ , with the mean anomaly at epoch,  $M_0 = M - nt$ , so that the state vector is  $[a, e, i, \Omega, \omega, M_0]$ . In this way, we remove the mean motion term from the equations of motion. We can choose the epoch time as the time of periapsis passage of the reference point, so that the time since epoch,  $t$ , is given by

$$t = \frac{M_{\text{ref}}}{n_{\text{ref}}} \quad (48)$$

and the desired mean anomaly at epoch,  $M_{0_{\text{ref}}}$  is always zero.

We complete the control derivation by defining a quadratic, positive-definite Lyapunov function:

$$V = \frac{1}{2} \left[ K_1 \frac{\delta a^2}{R_e^2} + K_2 \delta e^2 + K_3 \delta i^2 + K_4 \delta \Omega^2 + K_5 \delta \omega^2 + K_6 \delta M_0^2 \right] \quad (49)$$

Note that in Eq. (49), we assume a diagonal gain matrix,  $\mathbf{K}$ , and incorporate it into the Lyapunov function. Taking the derivative of the Lyapunov function with respect to the state,  $\mathbf{x}$ , we get

$$V_x = \left[ K_1 \frac{\delta a}{R_e^2} \quad K_2 \delta e \quad K_3 \delta i \quad K_4 \delta \Omega \quad K_5 \delta \omega \quad K_6 \delta M_0 \right] \quad (50)$$

Substituting into Eq. (44) yields the following classical orbital element Lyapunov control law:

$$\mathbf{u}_{\text{cl}} = -[\mathbf{g}(\mathbf{x})]^T V_x^T = - \begin{bmatrix} \frac{2a^2 e S \nu}{h} & \frac{2a^2 p}{hr} & 0 \\ \frac{p S \nu}{h} & \frac{(p+r)C\nu+re}{h} & 0 \\ 0 & 0 & \frac{rC(\omega+\nu)}{h} \\ 0 & 0 & \frac{rS(\omega+\nu)}{h} \\ -\frac{pC\nu}{he} & \frac{(p+r)S\nu}{he} & -\frac{hSi}{rS(\omega+\nu)Ci} \\ \frac{b(pC\nu-2re)}{ahe} & -\frac{b(p+r)S\nu}{ahe} & 0 \end{bmatrix}^T \begin{bmatrix} K_1 \frac{\delta a}{R_e^2} \\ K_2 \delta e \\ K_3 \delta i \\ K_4 \delta \Omega \\ K_5 \delta \omega \\ K_6 \delta M_0 \end{bmatrix} \quad (51)$$

This formation control law works well for low-thrust, multi-orbit maneuvering of spacecraft in non-circular, non-equatorial orbits. To find such a control for spacecraft in nearly circular or equatorial orbits, we first introduce the equinoctial element set, whose equations of motion contain no singularities.

The non-singular equinoctial elements are defined in terms of the classical orbital elements as:

$$a = a \quad (52)$$

$$P_1 = e \sin \varpi \quad (53)$$

$$P_2 = e \cos \varpi \quad (54)$$

$$Q_1 = \tan \frac{i}{2} \sin \Omega \quad (55)$$

$$Q_2 = \tan \frac{i}{2} \cos \Omega \quad (56)$$

$$l = \varpi + M \quad (57)$$

where  $\varpi$ , the longitude of pericenter, is defined as

$$\varpi = \Omega + \omega \quad (58)$$

In addition to the mean longitude,  $l$ , we also need the true longitude,  $L$ , defined as

$$L = \varpi + \nu \quad (59)$$

We can once again manipulate the mean longitude,  $l$ , to get the mean longitude at epoch,  $l_0$ , by replacing  $M$  with  $M_0 + nt$ :

$$l_0 = \varpi + M_0 = \varpi + M - nt = l - nt \quad (60)$$

Here we define epoch as the time where the reference mean longitude is zero, and thus the time since epoch is

$$t = \frac{l_{\text{ref}}}{n_{\text{ref}}} \quad (61)$$

Thus we remove the mean motion from the equations of motion of the longitude term. From Battin,<sup>30</sup> the equinoctial variational equations in a Gauss-like form are:

$$\dot{\mathbf{x}} = \begin{bmatrix} \frac{2a^2(P_2SL - P_1 \cos L)}{h} & \frac{2a^2p}{hr} & 0 \\ -\frac{pCL}{h} & r\left[P_1 + \left(1 + \frac{p}{r}\right)SL\right] & -\frac{P_2(Q_1CL - Q_2SL)r}{h} \\ \frac{p \sin L}{h} & r\left[P_2 + \left(1 + \frac{p}{r}\right)CL\right] & \frac{P_1(Q_1CL - Q_2SL)r}{h} \\ 0 & 0 & \frac{r(1 + Q_1^2 + Q_2^2)SL}{2h} \\ 0 & 0 & \frac{r(1 + Q_1^2 + Q_2^2)CL}{2h} \\ -\frac{pa\left[(P_1SL + P_2CL) + \frac{2b}{a}\right]}{h(a+b)} & -\frac{ra\left(1 + \frac{p}{r}\right)(P_1CL - P_2SL)}{h(a+b)} & -\frac{r(Q_1CL - Q_2SL)}{h} \end{bmatrix} \begin{bmatrix} u_r \\ u_\theta \\ u_h \end{bmatrix} \quad (62)$$

where the state  $\mathbf{x}$ , is the  $[6 \times 1]$  equinoctial element set,  $[a, P_1, P_2, Q_1, Q_2, l_0]$ , and where

$$b = a\sqrt{1 - P_1^2 - P_2^2} \quad (63)$$

$$h = nab \quad (64)$$

$$\frac{p}{r} = 1 + P_1 \sin L + P_2 \cos L \quad (65)$$

$$\frac{r}{h} = \frac{h}{\mu(1 + P_1 \sin L + P_2 \cos L)} \quad (66)$$

We choose a candidate Lyapunov function as:

$$V = \frac{1}{2} \left[ K_1 \frac{\delta a^2}{R_e^2} + K_2 \delta P_1^2 + K_3 \delta P_2^2 + K_4 \delta Q_1^2 + K_5 \delta Q_2^2 + K_6 \delta l_0^2 \right] \quad (67)$$

whose partial derivative with respect to the state,  $\mathbf{x}$ , is given by

$$V_x = \left[ K_1 \frac{\delta a}{R_z^2} \quad K_2 \delta P_1 \quad K_3 \delta P_2 \quad K_4 \delta Q_1 \quad K_5 \delta Q_2 \quad K_6 \delta l_0 \right] \quad (68)$$

Substituting into Eq. (44) yields the following equinoctial orbital element Lyapunov control law:

$$\mathbf{u}_{\text{eq}} = - \begin{bmatrix} \frac{2a^2(P_2SL - P_1CL)}{h} & \frac{2a^2p}{hr} & 0 \\ -\frac{pCL}{h} & \frac{r[P_1 + (1 + \frac{p}{r})SL]}{h} & -\frac{P_2(Q_1CL - Q_2SL)r}{h} \\ \frac{pSL}{h} & \frac{r[P_2 + (1 + \frac{p}{r})CL]}{h} & \frac{P_1(Q_1CL - Q_2SL)r}{h} \\ 0 & 0 & \frac{r(1 + Q_1^2 + Q_2^2)SL}{2h} \\ 0 & 0 & \frac{r(1 + Q_1^2 + Q_2^2)CL}{2h} \\ -\frac{pa[(P_1SL + P_2CL) + \frac{2b}{a}]}{h(a+b)} & -\frac{ra(1 + \frac{p}{r})(P_1CL - P_2SL)}{h(a+b)} & -\frac{r(Q_1CL - Q_2SL)}{h} \end{bmatrix}^T \begin{bmatrix} K_1 \frac{\delta a}{R_z^2} \\ K_2 \delta P_1 \\ K_3 \delta P_2 \\ K_4 \delta Q_1 \\ K_5 \delta Q_2 \\ K_6 \delta l_0 \end{bmatrix} \quad (69)$$

The classical and equinoctial Lyapunov control laws can both be scaled without further modification. Additionally, we can modify both of these control laws to exclude radial thrusting by setting the terms in the first column of the  $\mathbf{g}$  matrix to zero.

## SIMULATION AND RESULTS

Numerical simulation of typical maneuvers are presented to illustrate the effectiveness of these control laws. The primary method of simulation used here implements the  $f$  and  $g$  method<sup>31</sup> with impulsive  $\Delta v$ 's applied at one-second time intervals. This approach closely fits the application of pulsed plasma thrusters fired at 1 Hz.

We also use a continuous-time simulation to obtain time-optimal solutions for comparison with the feedback controllers developed here. Discretized thrust profiles resulting from the time-optimal solutions are implemented in the discrete  $f$  and  $g$  simulation.

The primary maneuver reported here is the case of an anomaly shift maneuver. The orbit chosen for the maneuver has

$$a = 6775 \text{ km} \quad (70)$$

$$e \approx 0 \quad (71)$$

$$i = 51.6^\circ \quad (72)$$

The maneuvering spacecraft starts in the same plane as the target orbit, but with an anomaly shift of  $\delta\nu = 10^{-4}$  radians (see Fig. 2). We illustrate the performance of the controllers using plots of the error dynamics and the thrust profiles, as well as impulse counts as a measure of fuel consumption.

The simulation calculates the inertial position and velocity of the spacecraft and target, and calculates a feedback control law defined in the preceding sections. Thrust is applied if the requested control magnitude is greater than the available thrust from the PPTs ( $112\mu N$ ). The simulation calculates and applies impulsive  $\Delta V$  at 1Hz, and propagates the resulting Keplerian motion using the  $f$  and  $g$  method.

The time-optimal solution assumes continuous thrust in the orbital plane, and results in a maneuver that takes 12,540 seconds (about 2.26 orbits). Note that the time-optimal solution does admit radial thrust; thus its performance could easily be substantially better than the feedback controllers that do not admit radial thrust. The time-optimal solution used as a baseline for comparison is shown in Fig. 5.

The LQR solution shown in Fig. 6 shows that the linear controller has similar performance to the time-optimal controller, but uses more propellant. Tuning of this controller would certainly improve its performance.

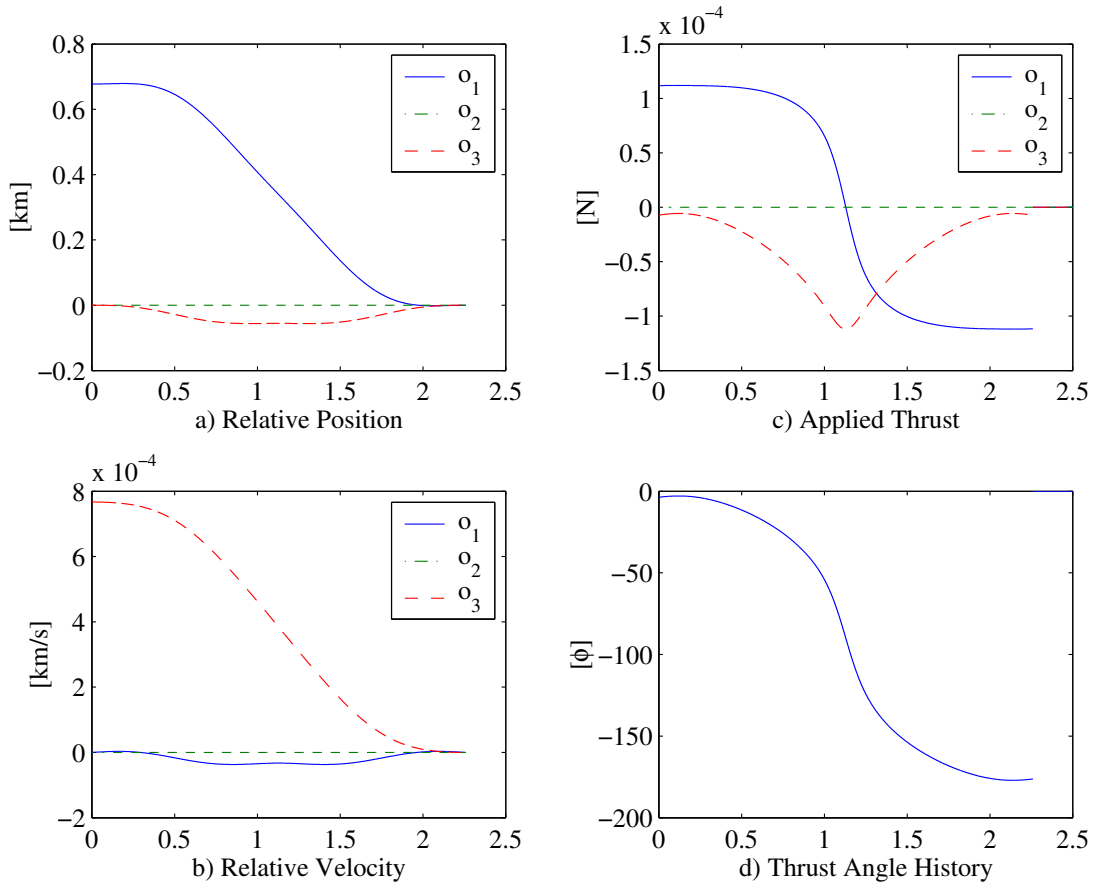


Figure 5: Time optimal continuous thrust solution, converges after 12,540 impulses

An example of the  $H_\infty$  controller is shown in Fig. 7. As with the LQR controller, the performance is similar to the time-optimal, but tuning is needed to obtain equivalent performance.

The equinoctial element controller results are shown in Fig. 8. Note that this controller performs almost as well as the time-optimal controller. This control allows us to exploit the fact that increasing the semi-major axis of the maneuvering spacecraft decreases its mean motion and thus performs a near-optimal anomaly shift maneuver. We accomplish this by defining a positive definite  $K$  matrix with  $(-)$  off diagonal  $K_{16}$  term. Because this is an upper triangular matrix, we can set the off diagonal term however we please without affecting the positive definiteness of the matrix. In this simulation, we begin with a finite  $K_{16}$  value, and set it to zero as soon as the mean longitude at epoch,  $l_0$ , is sufficiently small. In this case, we turn off the cross variable term when  $l_0 < 10^{-6}$  radians.

The performance characteristics of the four different controllers are summarized in Table 1. The table provides the number of impulses required to converge, the time to converge in orbital periods, and the ratio of the number of impulses required for the given controller over the number of impulses required by the time-optimal controller.

## CONCLUSIONS

Several state-feedback control techniques for the maneuvering and maintenance of a formation of satellites have been developed. These techniques are based both on linear and nonlinear representations of the state dynamics. A minimum-time continuous thrust control is presented as a

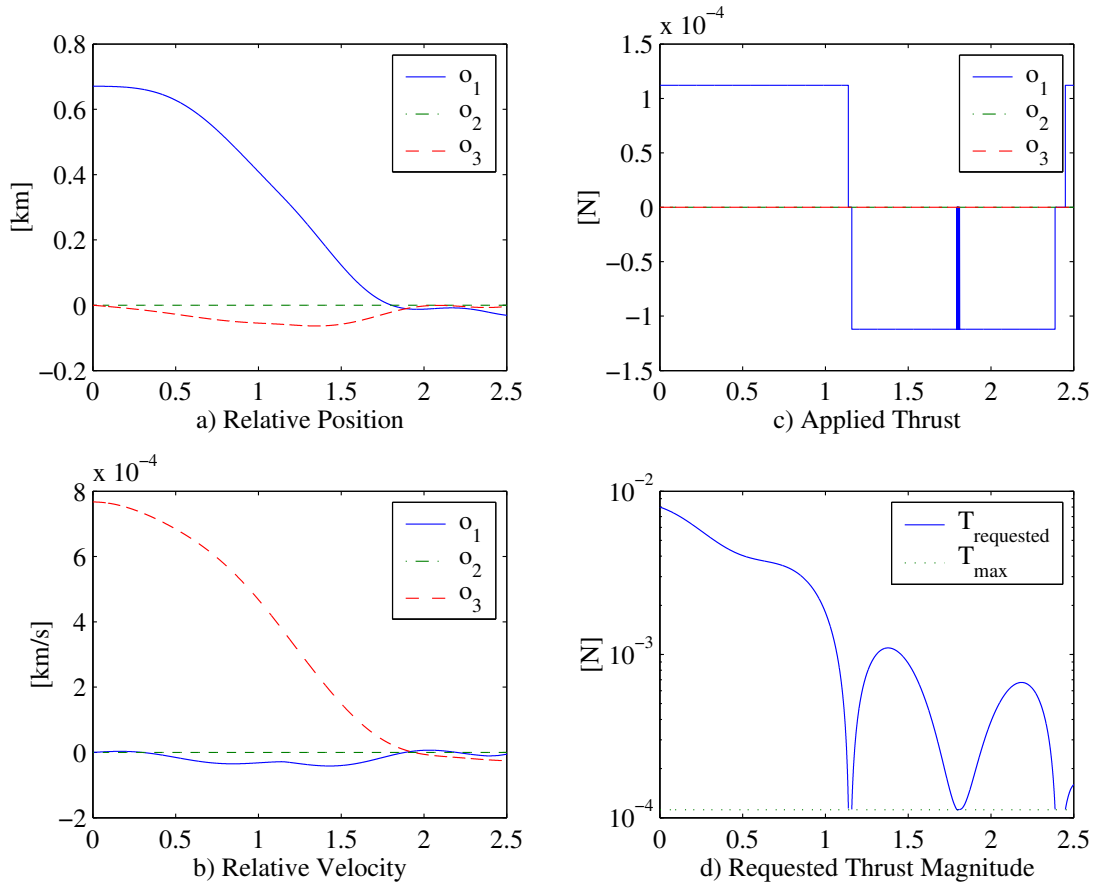


Figure 6: LQR control simulation, converges after 14,373 impulses

baseline for comparison. The linear controllers are based on the Hill-Clohessy-Wiltshire equations. Discrete-time  $H_2$ /LQR and  $H_\infty$  control solutions are presented. The nonlinear controllers are based on the Lyapunov control approach. Performance of the Lyapunov controller is nearly equivalent to that of the time-optimal control. Tuning of the equinoctial element-based Lyapunov control is facilitated by the physical insight into these states. However, the linear controllers are more difficult to tune, leading to inferior performance using the gains illustrated here.

## ACKNOWLEDGEMENTS

This work was supported by grants from the Air Force Office of Scientific Research and NASA Goddard Space Flight Center. The minimum-time continuous thrust solutions were obtained by

Table 1: Comparison of controller performance

Control law	Number of impulses	Orbits to converge	Dead zone amplitude (m)	Ratio of impulses to optimal
Optimal	12,540	2.26	0.2	1
LQR	14,373	4.35	5.2	1.15
$H_\infty$	15,803	4.31	6.7	1.26
Equinoctial	12,683	2.28	10.8	1.01

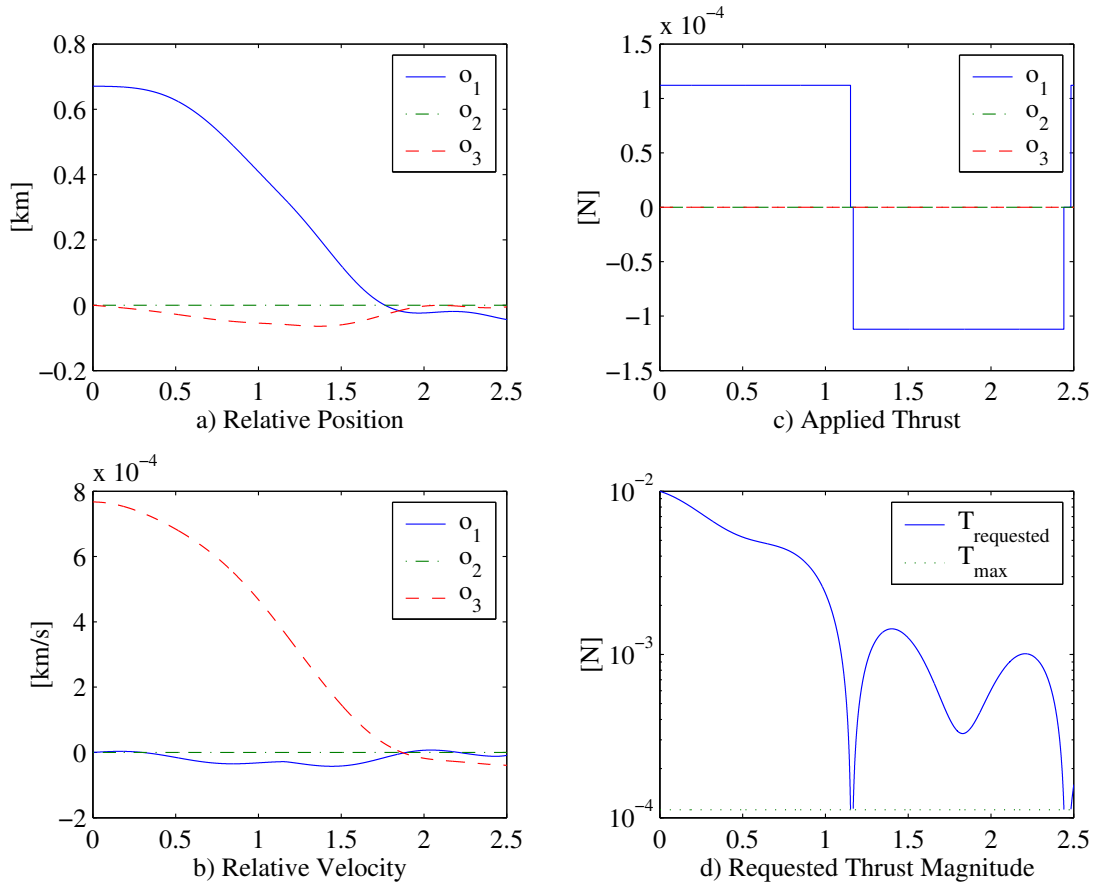


Figure 7:  $H_\infty$  control simulation, converges after 15,803 impulses

Victor Collazo-Perez, a graduate research assistant in Aerospace and Ocean Engineering at Virginia Tech.

## References

- [1] Hall, C. D. et al., "Virginia Tech Ionospheric Scintillation Measurement Mission," *Proceedings of the AIAA/Utah State University Conference on Small Satellites*, Logan, Utah, Aug 1999.
- [2] Campbell, M., Fullmer, R. R., and Hall, C. D., "The ION-F Formation Flying Experiments," *Proceedings of the 2000 AAS/AIAA Space Flight Mechanics Meeting*, Clearwater, Florida, Jan 2000.
- [3] Cassady, R. J., Hoskins, A. W., Campbell, M., and Rayburn, C., "A Micro-Pulsed Plasma Thruster for the Dawgstar Spacecraft," *Proceedings of the 2000 IEEE Aerospace Conference*, Big Sky, Montana, 2000.
- [4] Rayburn, C., Campbell, M., Hoskins, A. W., and Cassady, R. J., "Development of a Micro-PPT for the Dawgstar Nanosatellite," *Proceedings of the 2000 AIAA/ASME/SAE/ASEE Joint Propulsion Conference*, Huntsville, Alabama, 2000.
- [5] Makovec, K. L., Turner, A. J., and Hall, C. D., "Design and Implementation of a Nanosatellite Attitude Determination and Control System," *Proceedings of the 2001 AAS/AIAA Astrodynamics Specialists Conference*, Quebec City, Quebec, 2001.

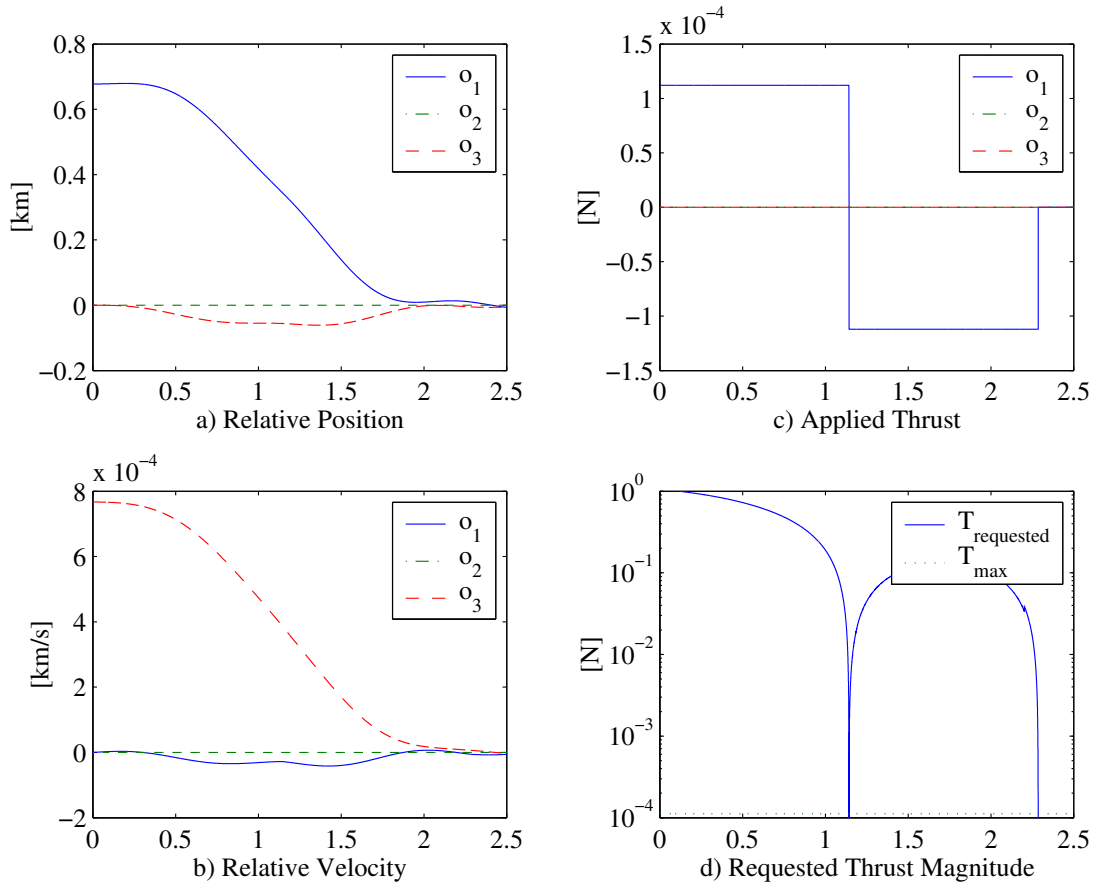


Figure 8: Equinoctial control simulation, converges after 12,683 impulses

- [6] Chacos, A. A., Stadter, P. A., and Deveraux, W. S., “Autonomous Navigation and Crosslink Communication Systems for Space Applications,” *Johns Hopkins APL Technical Digest*, Vol. 22, No. 2, 2001, pp. 135–143.
- [7] Stevens, C. L., Schwartz, J. L., and Hall, C. D., “Design and System Identification of a Nanosatellite Structure,” *Proceedings of the 2001 AAS/AIAA Astrodynamics Specialists Conference*, Quebec City, Quebec, 2001.
- [8] Vadali, S. and Vaddi, S., “Orbit Establishment for Formation Flying Satellites,” *Advances in the Astronautical Sciences*, Vol. 105, Part I, 2000, pp. 181–194, AAS 00-111.
- [9] Hughes, S. P. and Hall, C. D., “Optimal Configurations for Rotating Spacecraft Formations,” *Journal of the Astronautical Sciences*, Vol. 48, No. 2–3, 2000, pp. 225–247.
- [10] Schaub, H. and Alfriend, K. T., “Impulsive Spacecraft Formation Flying Control to Establish Specific Mean Orbit Elements,” *Journal of Guidance, Control, and Dynamics*, Vol. 24, No. 4, 2001, pp. 739–745.
- [11] Burl, J. B., *Linear Optimal Control*, Addison-Wesley, Reading, MA, 1999.
- [12] Vasser, R. H. and Sherwood, R. B., “Formationkeeping for a Pair of Satellites in a Circular Orbit,” *Journal of Guidance, Control, and Dynamics*, Vol. 8, No. 2, 1985, pp. 235–242.
- [13] Redding, D. C., Adams, N. J., and Kubiak, E. T., “Linear-Quadratic Stationkeeping for the STS Orbiter,” *Journal of Guidance, Control and Dynamics*, Vol. 12, No. 2, 1989, pp. 248–255.

- [14] Ulybyshev, Y., “Long-Term Formation Keeping of Satellite Constellation Using Linear-Quadratic Controller,” *Journal of Guidance, Control, and Dynamics*, Vol. 21, No. 1, 1998, pp. 109–115.
- [15] Carpenter, J. R., “Feasibility of Decentralized Linear-Quadratic-Gaussian Control of Autonomous Distributed Spacecraft,” *Flight Mechanics Symposium*, Goddard Space Flight Center, Greenbelt, MD, 1999.
- [16] Kluever, C. A. and Tanck, G. S., “A Feedback Guidance Scheme for Orbital Rendezvous,” *Journal of the Astronautical Sciences*, Vol. 47, No. 3/4, 1999, pp. 229–237.
- [17] Campbell, M. and Schetter, T., “Formation Flying Mission for the UW Dawgstar Nanosatellite,” *Proceedings of the 2000 IEEE Aerospace Conference*, Big Sky, Montana, 2000.
- [18] Kapila, V., Sparks, A. G., Buffington, J. M., and Yan, Q., “Spacecraft Formation Flying: Dynamics and Control,” *Journal of Guidance, Control and Dynamics*, Vol. 23, No. 3, 2000, pp. 561–564.
- [19] Sparks, A. G., “Satellite Formationkeeping Control in the Presence of Gravity Perturbations,” *Proceedings of the 2000 American Control Conference*, Chicago, Illinois, 2000.
- [20] Irvin, D. J. and Jacques, D. R., “A Study of Linear vs. Nonlinear Control Techniques for the Reconfiguration of Satellite Formations,” *Proceedings of the 2001 AAS/AIAA Astrodynamics Specialists Conference*, Quebec City, Quebec, 2001.
- [21] Clohessy, W. H. and Wiltshire, R. S., “Terminal Guidance System for Satellite Rendezvous,” *Journal of the Aerospace Sciences*, Vol. 27, No. 5, 1960, pp. 653–658, 674.
- [22] Karlgaard, C. D. and Lutze, F. H., “Second-Order Relative Motion Equations,” *AAS/AIAA Astrodynamics Specialists Conference*, Quebec City, Quebec, Canada, 2001, AAS 01-474.
- [23] Ogata, K., *Discrete-Time Control Systems*, Prentice-Hall, Englewood Cliffs, NJ, 1995.
- [24] Yaesh, I. and Shaked, U., “Minimum  $H_\infty$ -Norm Regulation of Linear Discrete-Time Systems and Its Relation to Linear Quadratic Discrete Games,” *IEEE Transactions on Automatic Control*, Vol. 35, No. 9, 1990, pp. 1061–1064.
- [25] Slotine, J.-J. E. and Li, W., *Applied Nonlinear Control*, Prentice-Hall, Englewood Cliffs, NJ, 1991.
- [26] Thomas Jr., N. B., *The Analysis and Control of Nonlinear Systems Using Lyapunov Stability Theory*, Master’s thesis, Virginia Polytechnic Institute and State University, Blacksburg, Virginia, 1996.
- [27] Brogan, W. L., *Modern Control Theory*, Prentice-Hall, Inc., Englewood Cliffs, NJ, 1985.
- [28] Schaub, H., Vadali, S. R., Junkins, J. L., and Alfriend, K. T., “Spacecraft Formation Flying Control Using Mean Orbital Elements,” *Advances in the Astronautical Sciences*, Vol. 103, Part 1, 1999, pp. 163–181, AAS 99-310.
- [29] Ilgen, M. R., “Low Thrust OTV Guidance Using Lyapunov Optimal Feedback Control Techniques,” *Advances in the Astronautical Sciences*, Vol. 85, Part 2, 1993, pp. 1527–1545, AAS 93-680.
- [30] Battin, R. H., *An Introduction to the Mathematics and Methods of Astrodynamics, Revised Edition*, American Institute of Aeronautics and Astronautics, Inc, Reston, VA, 1999.
- [31] Bate, R. R., Mueller, D. D., and White, J. E., *Fundamentals of Astrodynamics*, Dover, New York, 1971.